

A Distributed Infrastructure for Real-time Continuous VOC Monitoring in Hazardous Sites

Gianfranco Manes, Giovanni Collodi
 Francesco Chiti, Romano Fantacci
MIDRA Consortium
 Via di S.Marta 3, 50100 Florence, ITALY
 gianfranco.manes@unifi.it; giovanni.collodi@unifi.it
 francesco.chiti@unifi.it; romano.fantacci@unifi.it

Rosanna Fusco, Leonardo Gelpi
Health, Safety, Environment and Quality, eni SpA
 Piazzale E. Mattei, 1 00144 Rome, ITALY
 rosanna.fusco@eni.com; leonardo.gelpi@eni.com

Antonio Manes
Netsens Srl
 via Tevere 70, 50019 Sesto Fiorentino (FI), ITALY
 antonio.manes@netsens.it

Abstract—The real deployment is described of a distributed point source monitoring system based on wireless sensor networks in an industrial site where dangerous substances are produced, used and stored. The system consists of a Wireless Sensor Network using Photo-Ionisation Detectors, continuously monitoring the Volatile Organic Compound concentration in the petrochemical plant at unprecedented time/space scale. Internet connectivity is provided via TCP/IP over GPRS gateways at a one-minute sampling rate; thus, providing plant management and, possibly, environmental authorities with an unprecedented tool for immediate warning in case of critical events. The platform is organised into sub-networks, each including a gateway unit wirelessly connected to the WSN nodes, hence providing an easily deployable stand-alone infrastructure featuring a high degree of scalability and reconfigurability, with minimal intrusiveness or obtrusiveness. Environmental and process data are forwarded to a remote server and made available to the authenticated users through a rich user interface that provides data rendering in various formats and worldwide access to data. Experimental results show an excellent efficiency of the WSN system in terms of communication, making it a very flexible and cost-effective tool for environmental monitoring issues.

Keywords—distributed VOC monitoring; wireless sensor networks; photoionisation detectors.

I. INTRODUCTION

Volatile Organic Compounds (VOCs) are widely used in industries as solvents or chemical intermediates. Unfortunately, they include components that, if present in the atmosphere, may represent a risk factor for human health. VOCs are also found as contaminants or by-products in many processes, i.e., in combustion gas stacks and groundwater clean-up systems. Detection of VOCs at sub-ppm levels is, thus, of paramount importance for human safety, and, consequently, critical for industrial hygiene in hazardous environments [1][2]. The most commonly used portable field instruments for VOC detection are the hand-held Photo-Ionisation Detectors (PIDs), which may be fitted with pre-filter tubes for specific gas detection. Wireless hand-held PIDs have recently become available on the market, thus providing ubiquitous operation, but they have a limited battery life, in addition to being relatively costly. This paper describes the implementation and on-field results

of an end-to-end distributed monitoring system using VOC detectors, capable of performing real-time detection of gas emissions in potentially hazardous sites at minute data rate [3][4]. This paper describes the implementation of a distributed network for precise VOC monitoring installed in a potentially hazardous environment. The system consists of a WSN infrastructure with nodes equipped with weather-climatic sensors, as well as VOC detectors and fitted with TCP/IP over GPRS gateways to forward the sensor data via Internet to a remote server. The continuous monitoring of benzene emissions from a benzene storage tank is also demonstrated, using a unique wired/wireless configuration installed in ATEX Zone 0.

A user interface then provides access to the data, while offering various formats of data rendering. This prototype was installed in the eni Polimeri Europa (PEM) chemical plant in Mantova, Italy, where it has been in continuous and unattended operation since April 2011. The pilot site is currently testing and assessing both communications and VOC detection technologies.

II. SYSTEM OVERVIEW

A. The distributed VOC monitoring infrastructure

The distributed point sources method was chosen for this application as it provides reasonable installation and maintenance cost, a high scalability/reconfigurability and real-time data acquisition. A general overview of the deployed system is represented in Fig. 1.

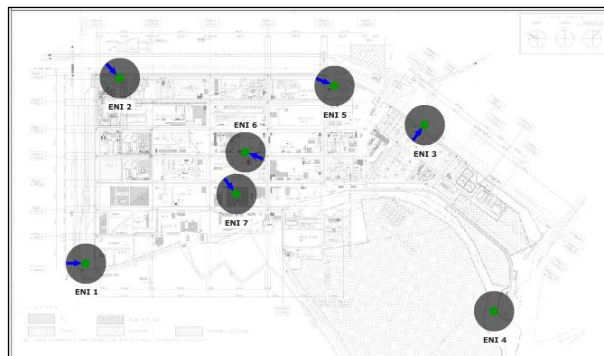


Figure 1. Installation overview; the grey circles indicate the position of each SNU; the blue arrows show wind direction.

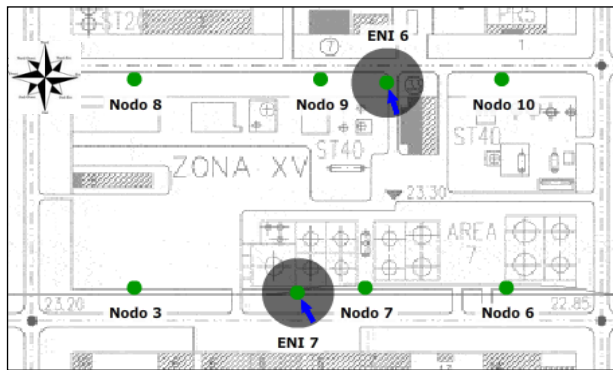


Figure 2. Close-up of SNU and ENU deployment around one of the chemical plants (left) and the pipeline (right); maps are oriented according to plant’s axes rather than cardinal directions.

First off, representative locations were identified along the perimeter of the industrial area, along with several specific internal sites where hazardous emissions might potentially occur. Owing to the extension and complexity of the Mantova plant, covering some 300 acres and featuring complex metallic infrastructures, it was decided to subdivide the area involved into 7 different sub-areas. Each sub-area is covered by a sub-network consisting of a Sink Node Unit (SNU) equipped with weather-climatic sensors, such as wind speed/direction and relative air humidity/temperature (ENI 1 to ENI 7 in Fig. 1), and End Node Units (ENUs) equipped with VOC detectors. In addition, the ENI 2 unit is equipped with a rain gauge and a solar radiation sensor.

Each SNU is connected to one or more ENUs (see Fig. 2, for an example of configuration), appropriately distributed across the plant area. This modular approach allows the system to be expanded and/or reconfigured according to the specific monitoring requirements, while providing redundancy in case of failure of one or more SNUs.

Since the potential sources of VOC emissions in the plant are located in well-identified areas, such as the chemical plant and the benzene tanks, the deployment strategy includes a number (6) of VOC sensors surrounding the chemical plant’s infrastructure, see Fig. 2, thus resulting in a virtual fence capable of effectively detecting VOC emissions on the basis of the concentration pattern around the plant itself. The SNUs forward meteorological data, as well as VOC concentration data, to a remote server; as noted above, Internet connectivity is provided via TCP/IP over GPRS using the GSM mobile network. Wireless connectivity uses the UHF-ISM unlicensed band. Electrical power is provided by both primary sources (batteries) and secondary sources (photovoltaic cells), as mentioned above.

VOC concentration and weather-climatic data are updated every minute. This intensive sampling interval allows the evolution of gas concentrations to be accurately assessed. Furthermore when all the weather-climatic measurements are collected, they provide a map of the relative air humidity/temperature (RHT) and wind speed/direction (WSD) in the area, that are crucial for providing accurate VOC-sensor read-out compensation [5].

The need for so many wind stations across the plant property is justified by the turbulent wind distribution in the area, as it can be observed by the different orientations of the blue arrows representing wind direction in Fig. 1.

Three of the ENUs, ENI 1, ENI 2 and ENI 3 were deployed along the perimeter of the plant to locally monitor VOC concentration while correlating it with wind speed and direction; the other seven were placed around the chemical plant and in close proximity of the pipeline, that are possible sources of VOC emissions.

In Fig. 2, the layout of the two sub-networks deployed around the chemical plant is represented. The sub-networks consist of two SNUs, ENI 6 and ENI 7, equipped with weather sensors (air/wind), each connected with three ENUs spaced at tens of meters from each other. The third sub-network located in the pipeline area consists of two ENUs located in close proximity of the end of the pipeline and connected to ENI 5. Sampling the VOC concentration at intervals of tens of meters allows the dispersion of VOC emissions to be evaluated; in addition, information about wind speed/direction allows the emission’s source to be identified.

B. Storage Tank monitoring infrastructure

Storage tanks represent a potential source of VOC emissions and, thus, need to be appropriately monitored. The emissions from tanks can vary significantly depending on the size and design, liquid properties, tank maintenance, tank level, wind direction, wind speed, and whether the tank is filling, stable, or emptying. Benzene storage tanks in this settlement are of floating roof type, and are located in highly hazardous areas; the electrical equipments to be operated in those areas need a special safety certification for use in potentially explosive atmospheres. Certification ensures that the equipment or protective system meets the safety requirements and that adequate information is supplied with it to ensure that it can be used safely.

The lay-out of the Storage Tank Monitoring Network (STMN) is displayed in Fig. 3. The STMN consists of three Volatile Organic Compound (VOC) units, each equipped with a Photo-Ionisation Detector (PID) and a computational unit, serially interconnected by wire and connected to the Wireless Unit (WU), providing both power and wireless connectivity.

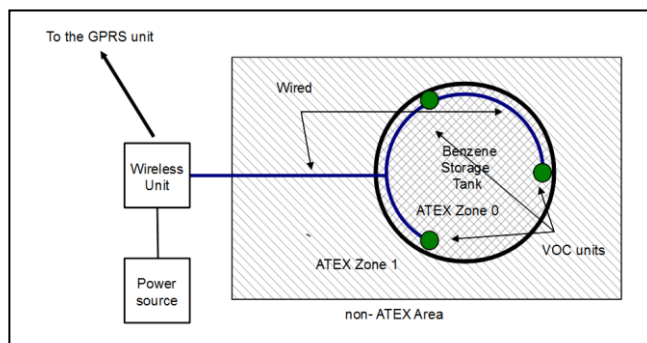


Figure 3. Schematic of the Storage Tank Monitoring Tank.

The WU is connected to the GPRS unit (ENI 3 in Fig. 1), which provides Internet connectivity via TCP/IP over GPRS.

The reason for choosing such a hybrid wired/wireless configuration is related to the VOC detector energy budget.

The PID, in fact, when operated at very low VOC concentration levels and in diffusion mode, requires to be continuously powered-on. Discontinuously operating the PID results in stabilisation times of the order of several tens of minutes for achieving a stable and reliable read-out.

That feature conflicts with the requirement of sampling the VOC concentration at minute data rates, a mandatory constrain for this application. Accordingly, it turns-out that the most suitable operation mode for the PID is the continuous power-on mode. In that mode, the current consumption for the VOC unit rises up to 50 mA, thus resulting in the need of a primary energy source with at least 80Ah capacity for ensuring a 60 days battery life; the requirement of bimonthly replacing 3 batteries on the top of the storage tank with skilled personnel was considered unpractical and too costly. On the other hand, the option of equipping the unit with a secondary energy source like a photovoltaic panel, thus prolonging the battery life, was discharged as it is hardly compatible with safety requirements of operation in ATEX Zone 0 and installation/maintenance above the benzene tank.

As a result, the hybrid configuration of Fig. 3 was envisaged, where the VOC units and communication/power supply units are split.

As it can be observed in Fig. 3, the three VOC detectors are located in Zone 0, very high level of protection, while the WU, along with the power unit consisting of the battery and the photovoltaic panel, is located in the non-ATEX area.

This allows for using a secondary energy source and for easily replacing the primary energy source as required by the maintenance programme.

III. THE COMMUNICATION PLATFORM

The distributed communications platform, already described [3][4], is able to support a scattered system of units collecting VOC emission data in real-time, while offering a high degree of flexibility and scalability, allowing for other monitoring stations to be added, as needed.

Furthermore, it provides reconfigurability, in terms of data acquisition strategies, while being more economically advantageous than traditional fixed monitoring stations.

A GSM mobile network solution featuring a proprietary TCP/IP protocol with DHCP, provides Internet connectivity. Dynamic re-connectivity strategies provide efficient and reliable communication with the GSM base station. All the main communication parameters, such as IP address, IP port (server's and client's), APN, PIN code and logic ID can be remotely controlled. Wireless connectivity between SNU's and ENU's is performed in the unlicensed ISM UHF band (868 MHz).

A. The SN and WI units

The block diagram of the SNU is represented in Fig. 4. It consists of a GPRS antenna, a GPRS/EDGE quadband modem, a sensor board, an I/O interface unit, and an ARM-9 micro-controller operating at 96 MHz.

The system is based on an embedded architecture with a high degree of integration among the different subsystems.

The unit is equipped with various interfaces, including LAN/Ethernet (IEEE 802.1) with TCP/IP protocols, USB ports and RS485/RS422 standard interfaces. The sensor board is equipped with eight analogue inputs and two digital inputs. The SNU is also equipped with a Wireless Interface (WI), shown in Fig. 4 right, which provides wireless connectivity with the ENU's.

B. The EN unit

The block diagram of the EN is shown in Fig. 5; it consists of a VOC sensor board and a VOC detector. The acquisition/communication subsystem of the ENU is based on an ARM Cortex-M3 32-bit micro-controller, operating at 72 MHz, which provides the necessary computational capability on the limited power budget available.

The block diagram of the ENU is shown in Fig. 5; it consists of a WI, similar to that previously described, and includes a VOC sensor board and a VOC detector. The acquisition/communication subsystem of the ENU is based on an ARM Cortex-M3 32-bit micro-controller, operating at 72 MHz, which provides the necessary computational capability on the limited power budget available.

To reduce the power requirement of the overall ENU subsystem, two different power supplies have been implemented, one for the micro-controller and one for the peripheral units.

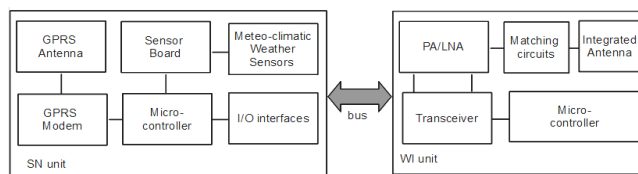


Figure 4. Block diagram of an SNU (left) and a WI unit (right).

The microcontroller is able to connect/disconnect the peripheral units, thus preserving the local energy resources.

The VOC detector subsystem is powered by a dedicated switching voltage regulator; this provides a very stable and spike-free energy source, as required for proper operation of the VOC detector itself.

The communication between the ENU and the VOC detector board is based on an RS485 serial interface, providing high-level immunity to interference as well as bidirectional communication capability, which is needed for remote configuration/re-configuration of the unit.

C. Network structure and routing schemes

A multiple GPRS gateway approach overcomes those limitations; even in the case of failure of one or more gateway units, Internet connectivity would be provided by the others still in operation, while the issue of the obstacles is circumvented.

Concerning the lower tier comprised of ENUs, it has been adopted the IEEE 802.15.4 standard to implement the communications features. This is motivated by the interoperability properties and flexibility when operating under different conditions [10]. In particular, the adopted MAC layer scheme follows the beacon enabled approach, in which a *coordinator* (SNU) periodically broadcasts a *beacon* packet for synchronizing the other nodes (ENUs) and arbitrating the access to the wireless shared medium through CSMA/CA protocol.

In designing the routing protocol, the IPv6 Routing Protocol for Low Power and Lossy Networks (RPL) has been adopted [11]. This recently standardized approach has been proposed to meet the forwarding requirements for Low Power and Lossy Networks (LNNs). In particular, RPL is a Distance Vector IPv6 routing protocol for LLNs that specifies how to build a Destination Oriented Directed Acyclic Graph (DODAG, sometimes referred to as a graph in the rest of this document) using an objective function and a set of metrics/constraints to prevent loops creation. The objective function operates on a combination of metrics and constraints to compute the ‘best’ path. There could be several objective functions in operation on the same node and mesh network because deployments vary greatly with different objectives and a single mesh network may need to carry traffic with very different requirements of path quality, involving, for example, latency, throughput, battery consumption or load balancing issues.

As for the wireless connectivity, a star configuration was preferred to a mesh configuration, given the limited number of nodes and the need to keep latency at a minimum.

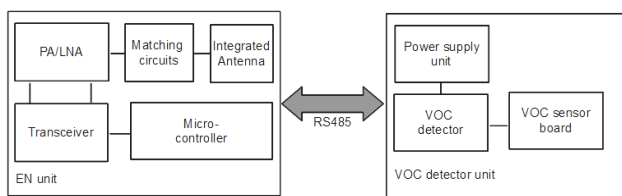


Figure 5. Block diagram of the ENU (left) and the VOC detector unit (right).

D. Protocols and WSN services

Two levels of communication protocols, in a mesh network topology, were implemented. The upper level handles communications between the SNUs and the server; it uses a custom binary protocol on top of a TCP layer. This level was designed and calibrated for real-time bidirectional data exchange, where periodic signalling messages are sent

from both sides. Since our sensor network necessitates a stable link, quick reconnection procedures, for whenever broken links should occur, were especially important. To ensure minimal data loss, the SNUs have non-volatile data storage, as well as automatic data packet retransmission (with timestamps) after temporary downlink events. Furthermore, this design is well suited for low-power embedded platforms like ours, where limited memory and power resources are available. In fact, our protocol stack currently requires about 24 KB of flash memory (firmware) and 8 KB RAM.

The lower level, in contrast to the upper one, concerns the local data exchange between the network nodes. Here a cluster tree topology was employed; each node, which both transmits and receives data packets, is able to forward packets from the surrounding nodes when needed. In this specific application, the topology and routing schemes are based on an ID assigned to each EN unit, where the ID can be easily adjusted using selectors on the hardware board. This choice allows for easy support and maintenance, even when non-specialized operators have to install, re-install or service one or more units.

E. Energy budget issues

Energy budget plays a key role in the maintainability of the WSN [6]. In our case, this is made even more critical by the necessity of providing stand-alone operation with periodic maintenance intervals exceeding four months.

Since electrical energy from the plant could not be used, secondary sources had to be locally available; photovoltaic panels (PVP) fit the bill. The SNUs are all equipped with PVPs, as they have to support a number of functions, including connectivity and data collection from sensors. The ENUs, when equipped with low-energy demanding sensors, have 3 to 5 years of battery life using primary sources. However, in this installation the ENUs have to support the power-hungry VOC sensors. For this reason, the ENUs are also equipped with PVPs.

The ENUs have been fully deployed since May 2011; since that time we have noticed that the VOC sensor energy budget is predominant compared to that of the computational/communication unit. This is a critical issue for the ENUs, as the PIDs used for reading the VOC concentration need to be continuously powered-on to operate efficiently. The actual current drawn by the PIDs resulted in some 30 mA, corresponding to 720 mAh a day, almost twice the amount required by the communication/computational units, ranging to some 360 mW a day. The ENU’s primary source capacity is 60 Ah, which provides more than 2 full months of continuous operation.

To rely on autonomous energy resources, while providing continuous operation, a secondary energy source was integrated into the ENU in order to supply the 360 mW+ 720 mW average power required. A 5 W photovoltaic

panel can fulfil the task only under ideal sunlight conditions, i.e., in summer, but hardly at all in winter. The photovoltaic power supply unit includes a charge regulator, which was specifically designed to provide maximum energy transfer efficiency from the panel to the battery under any operative condition. Great attention was paid to the design of the voltage regulator, as the secondary energy source plays a key role in ensuring the stand-alone and unattended operation of the communication platform.

Fig. 6 displays the battery voltage plots of the ENUs connected to SNU 1, 5 and 6. As it can be observed, the ENUs exhibit quite satisfactory charge conditions. ENU 10 (eni 6 nodo 10) exhibits a lower voltage level, probably due to a deployment in a partially shadowed area. For the other two ENUs, the battery voltage remains above a 11.6 V value, with a slight decreasing trend, in the period December 2011-January 2012. due to the lower solar energy because of the onset of wintertime.

F. The VOC detector

The VOC detector is a key element for the monitoring system’s functionality. For this application two criteria were considered mandatory. The first is that the VOC detector should be operated in diffusion mode, thereby avoiding pumps or microfluidic devices, which would increase the energy requirements and make the maintainability issues more critical. The second criteria was that the system should be able to operate in the very low part per billion (ppb) range, with a Minimum Detectable Level (MDL) of some 2,5 ppb with a $\pm 5\%$ accuracy in the 2,5 to 1000 ppb range, which represents the range of expected VOC concentration. The Photo-Ionisation Detector (PID) fulfils most of the above requirements [7][8].

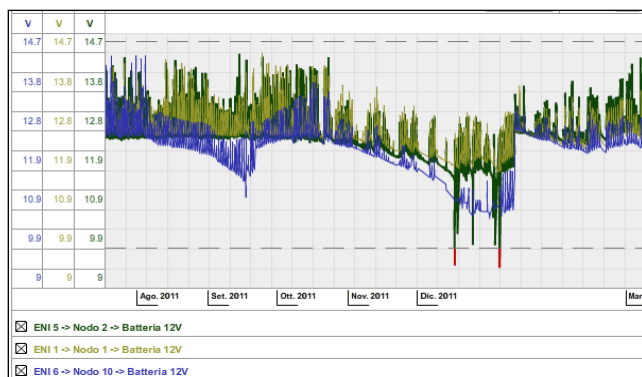


Figure 6. Battery voltage of the ENUs of the ENI 1, 5 and 6 sub-networks from July 18th 2011 to March 9th 2012.

A high sensitivity PID was chosen, featuring the specifications listed above [9]. Two major issues were identified; however, that could potentially affect the efficient use of the PID in our system. The first issue was that in the low ppb range the calibration curve of the PID

shows a marked non-linearity; this would require an individualized, meticulous multipoint calibration involving high cost and complexity. The second issue was that, when operated in diffusion mode at low ppb and after a certain time in power-off, the detector requires a stabilisation time of several minutes, hence it wouldn’t be able to operate at our required one-minute intervals.

Since both of the above-mentioned limitations are intrinsically related to the PID’s physical behaviour, this was carefully investigated and a behavioural model of the PID was developed to explain these phenomena. As a result, a mathematical expression of the PID calibration curve was derived. Accordingly, the PID calibration procedure could be performed by measuring only two parameters i.e., the zero gas voltage and the detector sensitivity in mV/ppm.

IV. EXPERIMENTAL RESULTS

A. Long term operation

Data gathered from the field are forwarded to a central database for data storage and data rendering. For this purpose, the system has a web based interface for retrieving and displaying data and for post-processing.

The interface features different formats to display the gathered data. It is possible both access to raw data, and generate summary reports relating to specific periods and specific network areas. All monitored parameters can be geo-referenced.

Data from the individual sensors deployed on the field, either micro-climatic or VOC, can be directly accessed and presented in various formats. Fig. 7 shows the VOC concentration read-out of one of the VOC detector deployed in the PEM settlement. The graph shows undiscontinued operation over a period of ten months (May 2011-March 2012); the background concentration value is below 150 parts per billion (ppb), as expected.

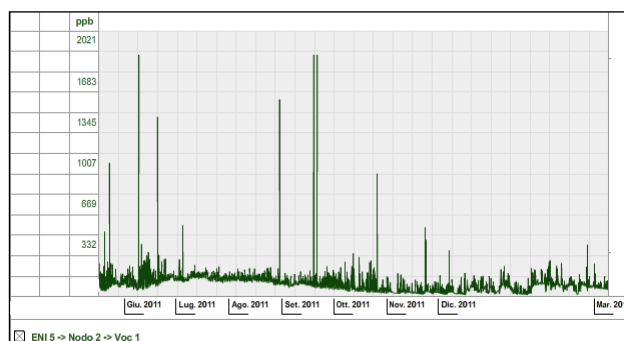


Figure 7. VOC concentration read-out during the period May 2011, March 2012.

The spikes observed in the graph are probably related to some operation and/or maintenance running in the plant.

Fig. 8 shows the trend of VOC concentrations values (detected by the six PIDs deployed around the chemical

plant) in a monthly period of almost two months (January 15th 2012-March 10th 2012). Background measured values are coherently comparable to each other, demonstrating the effectiveness of the calibration procedure.

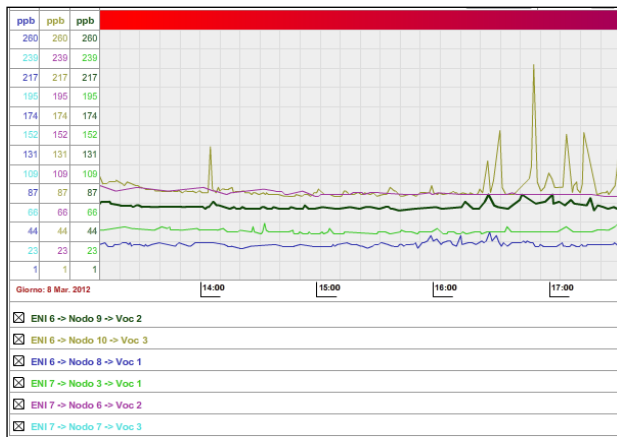


Figure 8. Graph of VOC concentration measured by six detectors deployed around the chemical plant (two months).

In Fig. 9, the VOC shows the concentration background, that is around 50 ppb; thanks to the very intensive sample-interval, 1 minute, the evolution of the concentration in time, along with other relevant meteorological parameters can be very accurately displayed; it should be noted that the spikes, which can be observed in the blue trace, Fig. 13 left, have a duration of some 3 minutes. The multi-trace graphic feature is very useful to perform correlation between different parameters.

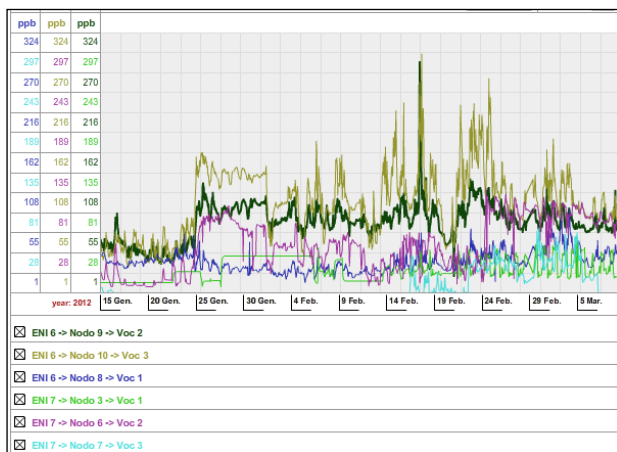


Figure 9. Graph of VOC concentration measured by six detectors deployed around the chemical plant (5 hours)

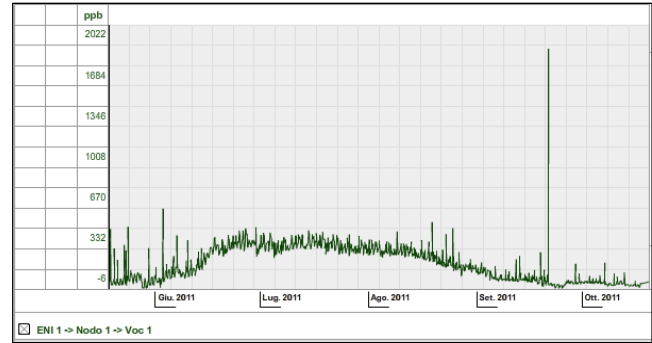


Figure 10. Graph of VOC concentration measured by a peripheral VOC detector over a period of four months.

Fig. 10 shows VOC concentrations in the long term (5 months) for a sensor positioned along the perimeter of the industrial area.

As it can be observed, data show an increase of the background value during the summer, due probably to higher temperatures.

Values tend to decrease from September. Peak value shown around 25th of September (concentration greater than 500 ppb) is due to meteorological conditions that may affect the dispersion of pollutants.

B. VOC concentration and weather-climatic variations

Correlating the microclimatic and wind parameters (air temperature/humidity and wind speed/direction) and VOC concentration proved to be very effective for increasing VOC read-out accuracy and, moreover, to map the VOC concentration with respect to wind direction, in order to identify possible VOC source.

When VOC sources need to be identified, in fact, the correlation between wind/speed direction and VOC concentration is vital. For this reason, a graphic representation that relates these two parameters can be very useful for interpretation of results.

An example of that possibility is given by the plots of Fig. 11. The graph represents the trend of VOC concentrations values (detected by the six PIDs deployed around the chemical plant) in a five days period.

With reference to the lay-out of Fig. 2, the VOC read-outs from the array deployed in the northern side of the plant are represented in Fig. 11 up, while the VOC read-outs from the array deployed in the southern side of the plant are represented in Fig. 11 down. The wind direction is also plotted in both the graphs of Fig. 11; it turns-out that in the most of the period the wind blows from south to north; By comparing the VOC read-out of the two arrays it is observed that the values of the former exhibits a much higher mean value than the latter; this is consistent with the direction north-south of the wind and demonstrates the effectiveness of the correlation between wind direction and speed to identify possible VOC sources.

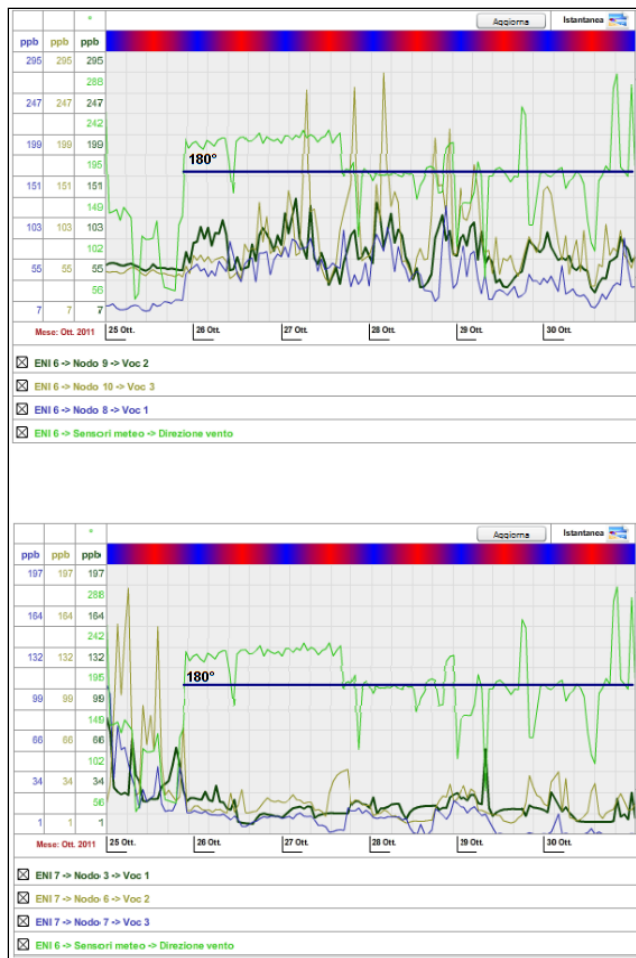


Figure 11. Source identification by correlation between VOC concentration read-outs and wind direction.

In Fig. 12 different representations of VOC concentrations combined with the wind direction data is shown for one of the detectors located on the left side of the plant perimeter, namely ENI 1.

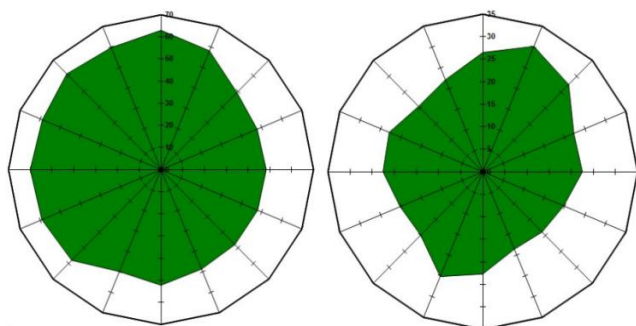


Figure 12. Plot in polar coordinates of the relationship between wind direction (angle) and concentration (radius).

The plot, in polar coordinates, represents the wind directions referenced to the North and the VOC

concentration in ppb. This type of representation allows to quickly identify the wind directions corresponding to the higher levels of concentration, giving an overview of the predominant orientation of the VOC flux during the day.

The plot in Fig. 12 left represents the concentration along 24 hours in a working day, while the plot in the right represents the same on a Sunday. As the detector eni 1 is located at the western side of the plant, see Fig. 1, it turns out that the concentration in the III and IV quadrants of the plot represents the contribution of the VOC sources outside the plant, while the concentration in the I and II quadrants represents the contribution of sources inside the plant.

Sources outside the plant are very likely the benzene emission by vehicles running on the motorway in direction North-South, along the western side of plant, or possible emissions from other industrial sites

Thermohygrometric parameters are useful to compensate for the air temperature/ relative humidity variations. Fig. 13 represents the typical relative response of PID as a function of temperature and relative humidity. It turns-out that, particularly in summertime, the climatic conditions in the plant can significantly affect the accuracy of the detected VOC concentration and need to be compensated for. This seems to be confirmed by the observation that the emissions in the III for IV decrease on Sunday, with respect to the working day, and by the highest value of the emission, 60 ppb in the left against 30 ppb in the right.

Fig. 14 shows the effect of thermohygrometric parameters on VOC detector read-out on three different VOC detectors located in the southern side of the chemical plant; see Fig. 2.

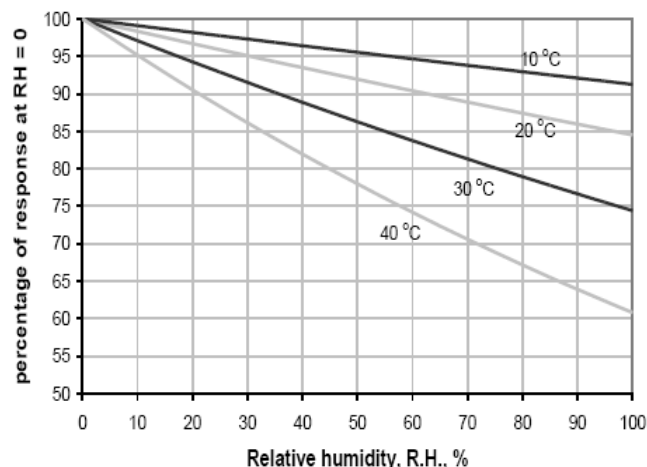


Fig. 13. VOC detector relative response as a function of thermohygrometric parameters (courtesy of Alphasense Ltd).

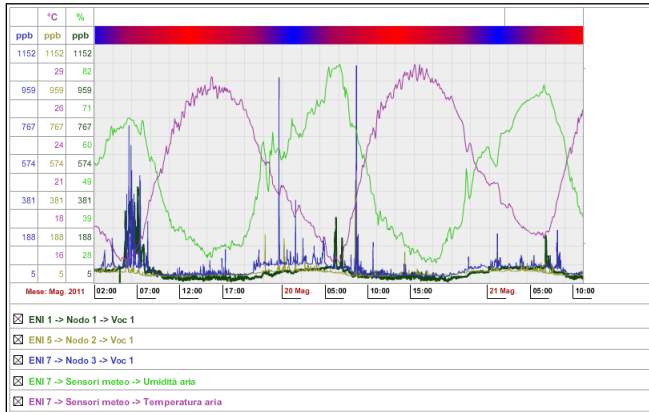


Figure 14. Correlation between air temperature/relative humidity and VOC detector read-out.

Maximum air temperature is as high as 30°C in the day, while air humidity reaches almost the 100% in the night. The predominant factor is the relative humidity; it is clearly observed that the VOC concentration values of all the three detectors follows the behaviour of the relative humidity, in accordance to what predicted by the plots of Fig. 13.

A post processing algorithm was implemented at the server side to compensate for the previously described effect. Fig. 15 shows the effect of the compensation, which results in smoothing the previously illustrated day/night effect.

C. Monitoring the benzene Tank

The network infrastructure displayed in Fig. 3 and previously described was operated starting from December 2011.

The VOC concentration recorded by the three detectors located on top the tank are plotted in Fig. 16, in the period December 11th 2011-March 15th 2012. The monitoring network installed in the proximity of the benzene storage tank roof proved to be very useful to identify and keep under control the process steps more significant in terms of emissions.

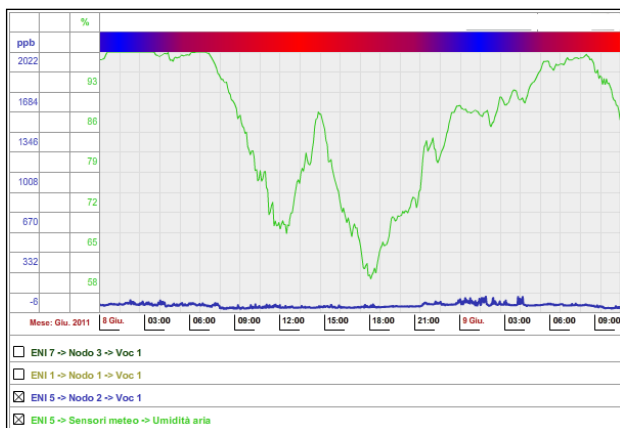


Figure 15. Compensation of the effect of thermohygrometric conditions.

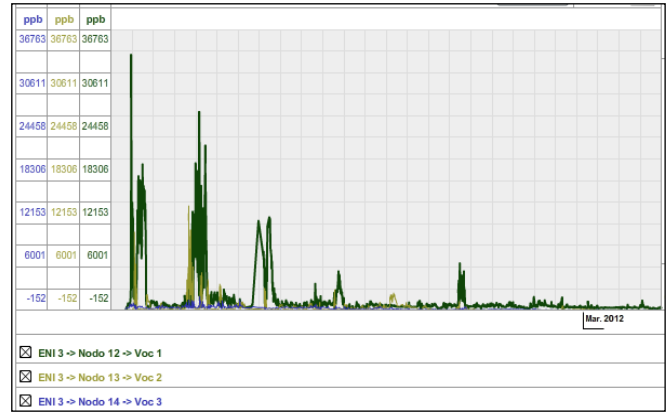


Figure 16. Graph of VOC concentration measured by three detectors deployed on top the benzene storage tank (December 11th 2011- March 15th 2012).

Periodic concentration peaks are observed, see Fig. 15, after complete filling of the tank; in such condition, the floating roof is located closer to the sensors and this allows to verify, along the perimeter of the roof, if there are sealing problems due to wear or deformation of the seals.

In the summer period the high volatility of the compounds could lead to variations in significant concentrations even during the emptying of the tank. The values found are in any case widely acceptable, since it is a direct emissions source.

D. Communications performance analysis

Before evaluating the performance of the proposed communications architecture, it has been addressed the available band the WSN is able to provide. In Fig. 17, a single-sink scenario where IEEE 802.15.4 nodes transmit data to the sink through one link (star topology), or possibly two-hops (3-level tree, rooted at the sink), is considered. A network composed of 30 nodes, working in beacon-enabled mode is accounted for. The throughput as a function of the size of the packets transmitted by nodes.

The throughput here represents the number of bits (of the payload) per second correctly received by the sink when all the 30 nodes try to access the channel and transmit their packets, assuming that nodes transmit packets of the same size.

It is possible to notice that, for low values of the packet size, star topology outperforms tree, whereas trees perform better when the packet size increases, since less nodes compete to access the channel at the same time (nodes are split in two levels). The optimal performance can be achieved for tree topology with super-frame order (SO) equal to zero and beacon order (BO) equal to two [10], which represents the best compromise between the duration of the active part of the sink super-frame (where level one nodes transmit) and that of the inactive part (where level 1 super-frames are located).

With the aim of characterizing the performance of the communications architecture proposed is presented, with

regard to the fault tolerance. As a matter of fact, the RPL protocol is able to update the routing tables, thus facing frequent disconnections and node failures.

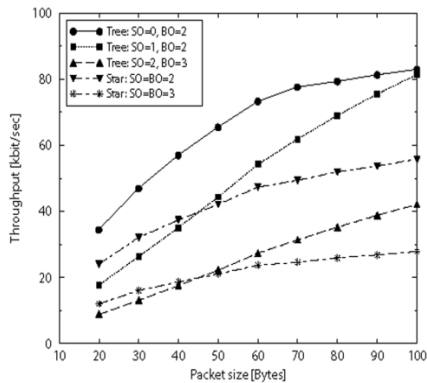


Figure 17. Throughput as a function of packet size for an IEEE 802.15.4 network arranged in star and tree-based topologies.

In deriving the key figures, three different scenarios have been investigated, as to the mobility, that has been assumed as the reason why the nodes get disconnected. The reference play-ground, that is a $800\text{m} \times 800\text{m}^2$ square area, with 4 SNUs deployed in fixed position, i.e., at the center of each of the four sub-squares, and 200 ENUs uniformly distributed. The differences consist in the mobility patterns, as it assumed for ENUs, respectively:

- No mobility;
- Random Way Point (RWP) mobility model with speed uniformly distributed in the interval [1-2] m/s (slow mobility);
- RWP mobility model with speed uniformly distributed in the interval [3-6] m/s (fast mobility).

For each scenarios the following figures of merit have been evaluated for the setup phase:

- Association efficiency, i.e., the number of ENUs that are connected with one SNU with respect to the total number of SNs;
- End-to-end (E2E) data delivery latency, i.e., the time interval needed to a data message to be received by correct ER;
- The length of established e2e paths (between an ENU and its SNU).

The most relevant simulation parameters, characterizing the communication links, are summarized in Tab. I.

TABLE I. PARAMETERS VALUES USED IN THE SIMULATIONS

Parameter	Value
Carrier Frequency [GHz]	2.4
Transmitted power [dBm]	0
Receiver sensitivity [dBm]	-110
Coverage radius [m]	≈ 80
Transmission Bit-rate [kb/s]	250
Packet error-rate [%]	5
Simulated time interval [s]	2000
Setup period [s]	3
Data period [s]	1

In Fig. 17, the association efficiency as a function of simulated time is depicted for each scenario. The initial transient time needed to reach a full network connectivity is very short due to the presence, in RPL of an explicit solicitation of DODAG information from the neighbors. As the network connectivity is achieved, data message can be delivered from ENUs to their respective SNUs. To evaluate the effectiveness of this phase, the E2E path length experimental cumulative distribution function (ECDF) has been outlined in Fig. 18. It is evident that RPL protocol is able to establish, maintain and exploit stable minimum hop paths. The proposed scheme is also able to face low-to-medium speed without significantly performance degradation, while for fast mobility pattern it no longer holds. Specifically, short E2E paths become more frequent while longer ones are more rare; this is due to the fact that a longer multi-hop path is not likely to be always guaranteed, because each ENU involved in can randomly move toward another area.

In Fig. 19, the E2E delivery time for a data message from an ENU to the reference SNU is presented again for three different mobility patterns. The robustness of RPL approach allows to keep latency below a reasonable value for low-to-medium speed range. Nevertheless, if SNs move more quickly, network get often disconnected and, as pointed out in Fig. 19, only shorter paths are stable during all the message delivering; thus, the E2E latency decreases.

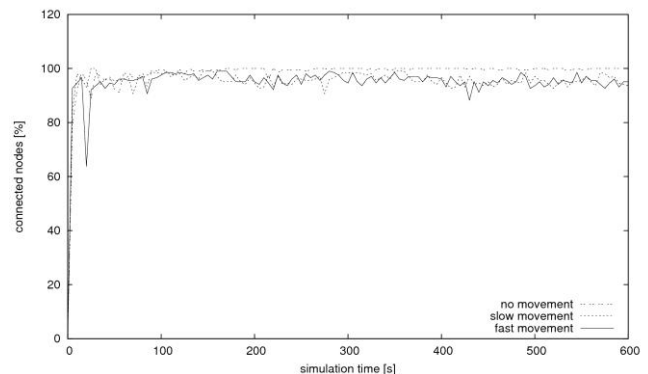


Figure 17. RPL: Association efficiency as a function of time.

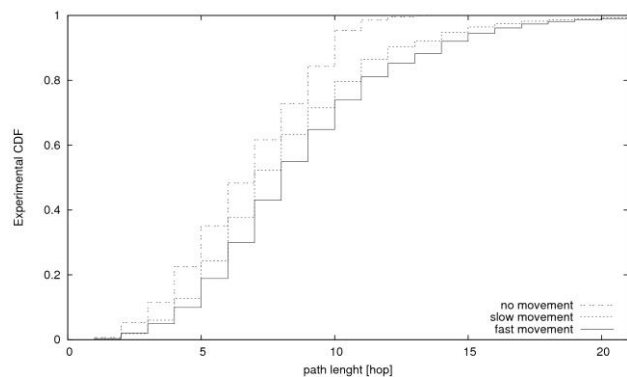


Figure 18. RPL: E2E path length CDF for different mobility pattern.

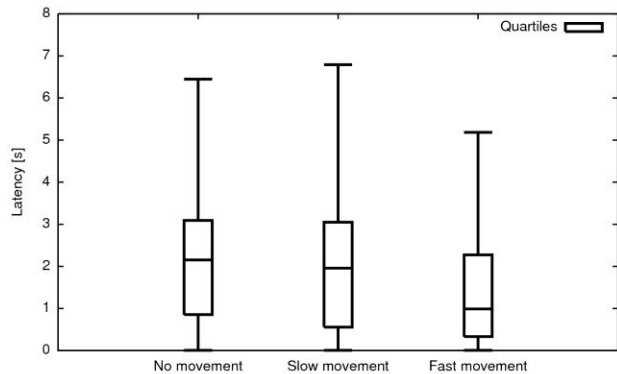


Figure 19. RPL: E2E data delivery latency for different mobility pattern with the indication of mean value and confidence interval.

V. CONCLUSION AND FUTURE WORK

An end-to-end distributed monitoring system of integrated VOC detectors, capable of performing real-time analysis of gas concentration in hazardous sites at an unprecedented time/space scale, has been implemented and successfully tested in an industrial site. The aim was to provide the industrial site with a flexible and cost-effective monitoring tool in order to achieve a better management of abnormal situations, to identify emission sources in real time, and to collect continuous VOC concentration data using easily re-deployable and rationally distributed monitoring stations.

The piloting of the system allowed us to pinpoint key traits. Collecting data at 1-minute time intervals meets several needs: identifying short-term significant events, quantifying the emission impacts as a function of weather conditions as well as of operational process, in addition to identifying potentially VOC sources in the plant area. Moreover, the choice of a WSN communication platform gave excellent results, above all in allowing for redeploying and re-scaling the network's configuration according to specific needs as they arise, while, at the same time, greatly reducing installation costs. Real-time data through a web-based interface allowed both adequate levels of control and quick data interpretation in order to manage specific situations.

Further developments will concern with the development of a standard application to allow the deployment of WSN in other plant (e.g., refineries), in addition to an assessment of potential applications for WSN infrastructure monitoring of other environmental indicators.

ACKNOWLEDGMENT

This work was supported by eni SpA under contract No. 3500007596. The authors wish to thank W. O. Ho and A. Burnley, at Alphasense Ltd., for their helpful comments and clarifications concerning PID operation, as well as E. Benvenuti, at Netsens Srl, for his valuable technical support. Assistance and support from the management and technical staff of Polimeri Europa Mantova is gratefully acknowledged.

REFERENCES

- [1] Tsujita W., Ishida H., and Moriizumi T. (2004), "Dynamic gas sensor network for air pollution monitoring and its auto-calibration," in *Proceedings of the IEEE Sensors*, Vol.1, pp. 56–59, October 2004.
- [2] Tsow F., Forzani E., Rai A., Rui W., Tsui R., Mastroianni S., Knobbe C., Gandolfi A.J., and Tao N.J. (2009), "A wearable and wireless sensor system for real-time monitoring of toxic environmental volatile organic compounds," in *Sensors Journal*, IEEE 9, Vol. 9 Issue 12, pp. 1734–1740, January 2009.
- [3] G. Manes, R. Fusco, L. Gelpi, A. Manes D. Di Palma and G. Collodi, "Real-time monitoring of volatile organic compounds in hazardous sites," in *Intech Book, Environmental Monitoring*, Chapter 14, pp. 219-244. ISBN 978-953-307-724-6.
- [4] G. Manes, R. Fusco, L. Gelpi, A. Manes D. Di Palma and G. Collodi, "A Wireless Sensor Network for Precise Volatile Organic Compound Monitoring," in *International Journal of Distributed Sensor Networks*, Special Issue on Ubiquitous Sensor Networks and Its Application. To appear.
- [5] MiniPID User Manual V1.8. (2000). IonScience Ltd.
- [6] G. Manes, R. Fantacci, F. Chiti, M. Ciabatti, G. Collodi, D. Di Palma, and A. Manes (2009), "Energy efficient MAC protocols for wireless sensor networks endowed with directive antennas: A cross-layer solution," in *Proceedings of IEEE Radio and Wireless Conference 2009*, pp. 239-242, Orlando, FL, January 2009.
- [7] Price JGW, Fenimore DC, Simmonds PG, and Zlatkis A. (1968), "Design and operation of a photoionization detector for gas chromatography," in *Analytical Chemistry*, Vol. 40, No. 3, March 1968, pp. 541-547.
- [8] Locke DC. and Meloan CE. (1965), "Study of the photoionization detector for gas chromatography," in *Analytical Chemistry*, Vol. 37, No. 3, March 1965, pp. 389-395.
- [9] Alphasense Ltd. Technical specifications; Doc. Ref. PID-AH/MAR11.
- [10] "IEEE Standard for Information Technology - Telecommunications and Information Exchange Between Systems - Local and Metropolitan Area Networks Specific Requirements Part 15.4: Wireless Medium Access Control (MAC) and Physical Layer (PHY) Specifications for Low-Rate Wireless Personal Area Networks (LR-WPANs)," IEEE Std 802.15.4-2003, pp. 1–670, 2003.
- [11] L. Bartolozzi, F. Chiti, R. Fantacci, T. Pecorella, F. Sgrilli, "Supporting Monitoring Applications with Mobile Wireless Sensor Networks: the 'eN Route' Forwarding Approach", in *Proc. IEEE ICC 2012*.